



BEHAVIOUR OF METAL MATRIX SYNTACTIC FOAMS UNDER CYCLIC LOADING

¹KATONA Bálint, ^{2,3}SZEBÉNYI Gábor PhD, ^{1,3}ORBULOV Imre Norbert PhD

¹Budapest University of Technology and Economics, Faculty of Mechanical Engineering, Department of Materials Science and Engineering

E-mail: katona@eik.bme.hu

²Budapest University of Technology and Economics, Faculty of Mechanical Engineering, Department of Polymer Engineering

E-mail: szebenyi@pt.bme.hu

³Budapest University of Technology and Economics, Faculty of Mechanical Engineering, MTA–BME Research Group for Composite Science and Technology

Abstract

Metal matrix syntactic foams consisting of aluminium alloys and oxide ceramic hollow spheres were investigated under compressive cyclic loading with load asymmetry factor of 0.1. The results ensured full reliability design data for the investigated material in the lifetime region, while the fatigue limits were determined by staircase method. The Wöhler curves of the foams were also constructed, including the median curves, their confidence boundaries and the fatigue strength. The softer Al99.5 matrix ensured higher load levels for the fatigue strengths than the more rigid AlSi12matrix. Considering the size of the ceramic hollow spheres, the large spheres with thick wall performed better than the more vulnerable smaller ones with thinner wall. The general failure mode was identified as a cleavage along a well determined shear band, similar to the case of quasi-static loading.

Keywords: metal matrix syntactic foams, composites, fatigue, cyclic loading.

1. INTRODUCTION

High strength, closed cell metallic foams, as ceramic hollow sphere reinforced metal matrix syntactic foams (MMSFs) are promising materials to build lightweight structural parts. Their can range from load bearing structures to vibration damping structural parts etc. In such cases, their fatigue properties are needed for proper design calculations.

The mechanical properties of MMSFs have been widely studied. The publications focus mainly on the compressive behaviour of the foams, but tensile and wear properties [1, 2] as well as structure reconstruction methods [3] have been published too. For example, the compressive properties of Al-Al₂O₃ MMSFs at different loading rates were monitored and predicted considering the strength of the matrix material and the size of the hollow spheres [4-6]. Other researchers [7-10] characterized glass microsphere reinforced iron based syntactic foams. Besides their production, the quasi-static mechanical properties and the strain-rate dependency of these them were investigated up to 10³ s⁻¹). The strain-rate influence observed for the MMSFs was mainly connected to the matrix. Taherishargh et al. [11, 12] provided cost effective production method by using low-density perlite as filler material. Because of the high porosity of the filler (~95%), the porosity of the foam was ~60%. Under compression, these MMSFs showed common stress–strain curves consisting of elastic, plateau and densification regions. Because of their consistent plateau stress (average value ~30 MPa), large densification strain (almost 60%), and high-energy absorption efficiency (~90%)

the produced MMSFs are effective energy absorbers. Besides the above mentioned and similar works, only a moderate effort was focused on the fatigue properties.

Vendra et al. studied the fatigue behaviour of different MMSFs that built up from steel hollow spheres in aluminium matrix (gravity casting) or in steel matrix (powder metallurgy). Under cyclic compressive loading, the MMSFs showed high cyclic stability and the deformation of the composite foam samples could be divided into three stages – linear increase in strain with fatigue cycles (stage I), steady state section with minimal strain accumulation in large number of cycles (stage II) and rapid strain accumulation within few cycles up to complete failure (stage III) [13].

2. METHODS

Standard Al99.5 and AlSi12 alloys were applied as matrix materials, while Globocer (GC) grade ceramic hollow spheres were applied as filler, provided by Hollomet GmbH. [14]. The material of the hollow spheres consists of 38 wt% Al_2O_3 , 43 wt% SiO_2 and 19 wt% $3\text{Al}_2\text{O}_3 \cdot 2\text{SiO}_2$. The hollow spheres show a normal distribution regarding their diameter ($1425 \pm 42 \mu\text{m}$) and wall thickness ($60 \pm 1.7 \mu\text{m}$), while their density is 0.816 gcm^{-3} . The amount of the filler material was maintained at ~65 vol%. The MMSFs were produced by pressure infiltration. During the infiltration 400 kPa infiltration pressure was applied for the infiltration time of 30 s. The infiltration temperature was always set to 50°C above the melting temperature of the matrix materials (660°C for Al99.5 and 575°C for AlSi12). The produced foams were designated after their constituents, for example Al99.5-GC stands for an MMSF sample with Al99.5 matrix and ~65 vol% of Globocer filler material. Cylindrical samples with diameter of $\varnothing 8.5 \text{ mm}$ and height of 12.75 mm (1.5 aspect ratio) were machined from the produced blocks. For classic fatigue tests, load levels (k) should be determined, that describe the maximum load (σ_{\max}) during each fatigue cycle in a relation to a limit strength. In the case of conventional metals, the load levels are usually related to the proof strength ($R_{p0.2}$) that is measured by simple tensile tests. In the case of MMSFs the proof strength can be substituted by the compressive strength (σ_c , the first local maximum in the engineering compressive stress – strain diagram, that causes irreversible failure, see Fig. 1).

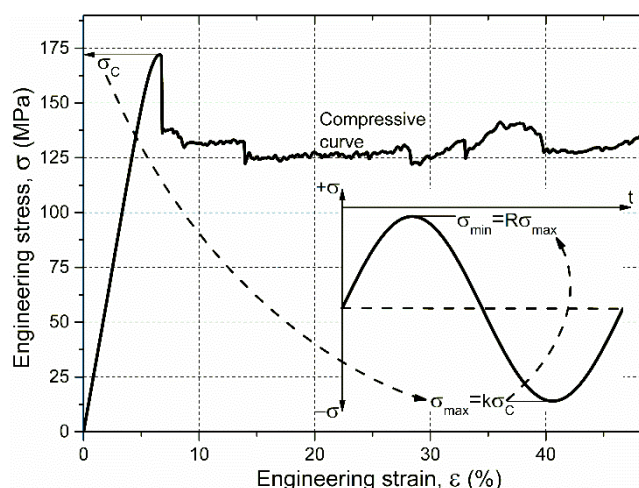


Figure 1 Typical quasi-static compressive curve of MMSFs and the derivation of the cyclic loading parameters σ_{\min} and σ_{\max} (inset figure)

The compressive strength (σ_c) of the foams, was measured for each material type on six samples (Table 1). On this basis the load levels can be defined as the ratio of the maximal load and compressive strength within the loading cycle (Eq. 1) and expresses similar load intensity, for the investigated materials that may have different compressive strength.

$$k = \frac{\sigma_{\max}}{\sigma_c} 100 (\%) \quad (1)$$

In our case the load level was altered between 60-100%. Fatigue tests were performed on an Instron 8872 type closed loop servo-hydraulic testing machine under force control and in compression-compression mode (stress asymmetry factor of $R=0.1$). The frequency of the fatigue tests was set to $f=10$ Hz and the load form followed a sine curve (inset of *Fig. 1*). The cylindrical specimens were carefully lubricated and placed between hardened and polished plates in a four bar upsetting tool.

Table 1 Compressive strength, sample number and time

Foam	Compressive strength, σ_c (MPa)	Number of samples at load level			SUM
		k=80%	k=85%	k=90%	
Al99.5-GC	19.7	3	9	9	
AlSi12-GC	40.0	9	9	9	
Overall number of samples		12	18	18	48
Overall number of cycles		6966673	28377	3320	6998370
Overall duration of tests (hours)		193.52	0.79	0.09	194.40

3. RESULTS

During the fatigue tests, the maximum values of the compressive engineering deformation were recorded in the function of cycles (*Fig. 2*). The curves can be divided into two parts. In stage I, the strain remains relatively constant over a large number of cycles. This stage is known as incubation period. A higher load ratio increases the overall strain in stage I. Stage II is accompanied by densification of the material and a rapid strain accumulation after a critical number of cycles. Higher load ratios shift the onset of stage II towards lower numbers of cycles.

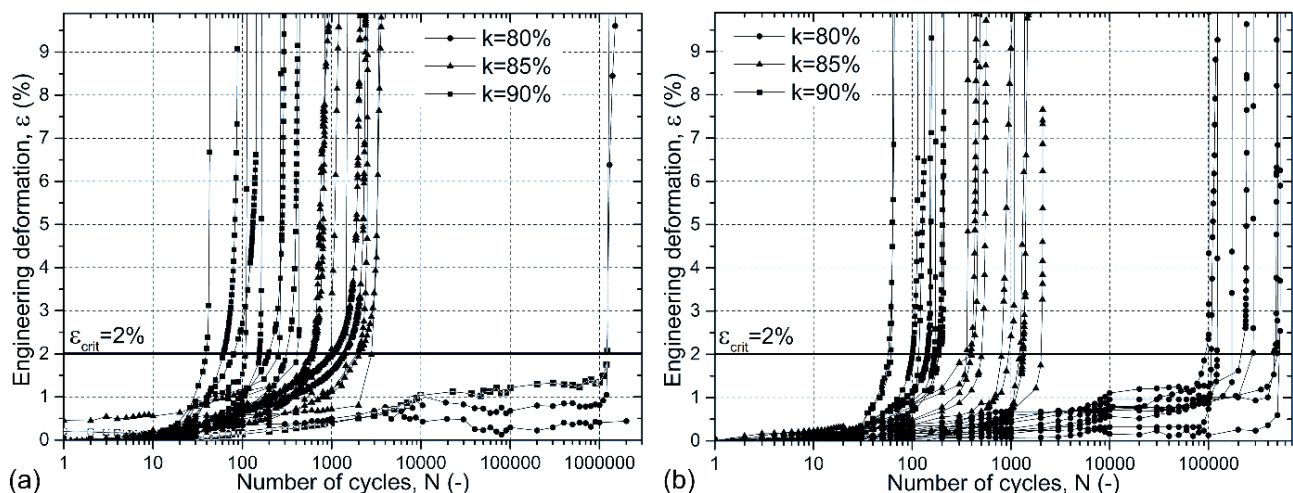


Figure 2 The measured compressive engineering deformation – number of cycles curves of (a) Al99.5-GC and (b) AlSi12-GC

For the correct evaluation of the deformation – cycle curves a failure criterion needs to be defined, that is always depending on the desired application. As there is no conventional criterion limit for the failure, the obtained deformation – number of cycle curves were evaluated at an arbitrarily chosen $\varepsilon_{\text{crit}}=2\%$ (*Fig. 2a*) in order to get the failure cycles (N_F). It should be emphasized that

$\varepsilon_{crit}=2\%$ engineering deformation corresponds to a macroscopically observable failure in the specimen. The obtained failure cycles showed large scatter, as it is usual in the case of fatigue test, therefore mathematical statistics, namely the Weibull distribution function (Eq. 2) was used to determine the expected number of cycles up to failure at a survival level (or probability, P_S) of 50%.

$$P_S = 1 - e^{-\left(\frac{N-N_0}{\alpha}\right)^\beta} \quad (2)$$

Where N is the independent variable, for which the equation should be evaluated to get the number of cycles up to the failure, N_0 is the threshold parameter, α is the scale parameter and β is the shape parameter of the function.

The next step is to construct the Wöhler-curve of the materials, that consists of two main parts. The first, endurance (or finite lifetime) part establish a relationship between the load level and the expected lifetime of the material. The second part represents the fatigue strength of the material. Considering the first part, the above derived results of the described mathematical statistic method are valid for the endurance range and the fitted line on them represents the endurance part of the Wöhler curve. By using this curve in the case of a given part and a given loading, the expected lifetime of the part can be predicted at the 50% survival probability (P_S).

Regarding the second part, the load level corresponds to the fatigue strength can be determined by the staircase method. First, the load level corresponds to the mean fatigue limit has to be estimated, and a fatigue life test is then conducted at a little higher load level than the estimated mean. If the specimen fails prior to the life of interest ($2 \cdot 10^6$ cycles in our case), the next specimen has to be tested at a somewhat lower load level. If the specimen does not fail within this life of interest, a new test has to be conducted at a higher stress level. Therefore, each test depends on the previous test results, and the test continues with a load level increased or decreased. The load level increments are usually taken to be less than about 5% of the initial estimate of the mean. The staircase method resulted in the load levels of 78.44% and 73.75%, that corresponds to the fatigue strength of 15.45 MPa and 29.50 MPa for the Al99.5-GC and AlSi12-GC MMSFs, respectively.

In the possession of the finite lifetime data and fatigue limit it is possible to construct the Wöhler curves of the MMSFs (Fig. 3). In Fig. 3 the measured points are shown by hollow squares, while the evaluated points are designated by black squares.

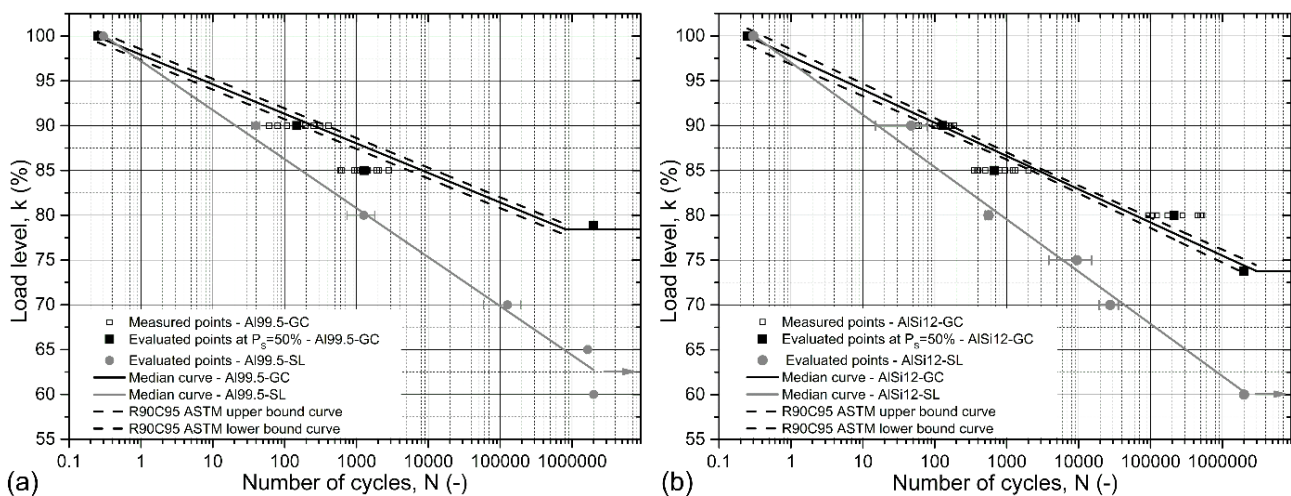


Figure 3 Wöhler curve for Al99.5-GC (a) and AlSi12-GC (b) MMSFs

The endurance part start from $k=100\%$ as that correspond to a single ($1/4$ cycle) uploading to the compressive strength. In the finite lifetime region, the black line was fitted on the evaluated points



INTERNATIONAL SCIENTIFIC CONFERENCE ON ADVANCES IN MECHANICAL ENGINEERING

13-15 October 2016, Debrecen, Hungary



by the least square method ($R^2=0.976$ and $R^2=0.978$ for the Al99.5-GC and AlSi12-GC foams, respectively). The load levels corresponding to the fatigue limits and obtained by the staircase method are also plotted by black line in the diagrams. The finite lifetime regions are supplemented by 90% reliability bands at 95% confidence level according to the ruling ASTM method (black dashed lines) [15]. Considering the identical scales and comparing Figs. 3a and 3b the technical purity Al99.5 matrix material ensured higher fatigue limit and higher lifetimes for a given load level. This phenomenon can be explained by the more or less pronounced rigidity of the high Si content eutectic Al matrix and by the presence of the Si lamellae in the matrix resulting in a moderate stress concentrating effect. On the other hand, the more ductile and soft technical purity Al matrix could hinder the incidental crack propagations resulting in a higher lifetime. These curves can be directly used to predict the expected lifetime of the MMSF parts based on their maximum permitted loading during operation, that could be determined by measurements on actual parts or can be estimated by finite element methods.

For comparison and to investigate the size effect of the hollow spheres preliminary measurements on MMSFs reinforced by smaller hollow spheres with identical chemical composition were performed. The smaller hollow spheres are commercially available under the SL300 grade name (provided by Envirospheres Pty. Ltd. [16], designated by SL in the diagrams). The average diameter ($150\pm 4.1\text{ }\mu\text{m}$) and wall thickness ($6.75\pm 0.2\text{ }\mu\text{m}$) of the smaller, SL grade hollow spheres were about one tenth of the GC grade spheres, while their density was slightly lower (0.691 gcm^{-3}). The preliminary tests were performed on fewer samples and the results were evaluated by simpler statistics (average and scatter). However, two important trends can be clearly observed: (i) in the case of the smaller hollow spheres similar relationship can be seen regarding the matrix material: the softer Al99.5 matrix ensured higher expected lifetimes at certain load levels and (ii) the lifetime region of the smaller spheres always run well below the curves of the GC spheres.

CONCLUSIONS

From the above investigations and analysis of the MMSFs, the following conclusions can be drawn:

- The Wöhler curve of the hollow sphere reinforced MMSFs were constructed according to the ruling ASTM standard for the case of compressive cyclic loading. The results include the median curves, their 95% confidence boundaries and the fatigue strength.
- The softer, technical purity Al99.5 matrix ensured higher load levels for the fatigue strengths than the more rigid, eutectic AlSi12 matrix.
- Regarding the size of the reinforcing ceramic hollow spheres, the larger, GC grade spheres performed better, because the smaller spheres are more vulnerable and the cracks have to propagate shorter distances within the ductile matrix to the next rigid ceramic sphere.

ACKNOWLEDGEMENTS

This paper was supported by the János Bolyai Research Scholarship of the Hungarian Academy of Sciences (Imre Norbert ORBULOV, Gábor SZEBÉNYI).

REFERENCES

- [1] Májlínger, K., Bozóki, B., Kalácska, G., Keresztes, R., Zsidai, L.: *Tribological properties of hybrid aluminum matrix syntactic foams*. Tribology International, 99, 211-223., 2016.
- [2] Májlínger, K.: *Wear properties of hybrid AlSi12 matrix syntactic foams*. International Journal of Materials Research. 106(11), 33-37., 2015.



INTERNATIONAL SCIENTIFIC CONFERENCE ON ADVANCES IN MECHANICAL ENGINEERING

13-15 October 2016, Debrecen, Hungary



- [3] Kozma, I., Zsoldos, I., Dorogi, G., Papp, S.: *Computer tomography based reconstruction of metal matrix syntactic foams*. Periodica Polytechnica Mechanical Engineering, 58, 87-91., 2014.
- [4] Santa Maria, J. A., Schultz, B. F., Ferguson, J. B., Rohatgi, P. K.: *Al-Al₂O₃ syntactic foams - Part I: Effect of matrix strength and hollow sphere size on the quasi-static properties of Al-A206/Al₂O₃ syntactic foams*. Materials Science and Engineering A. 582, 415-422., 2013.
- [5] Ferguson, J. B., Santa Maria, J. A., Schultz, B. F., Rohatgi, P. K.: *Al-Al₂O₃ syntactic foams - Part II: Predicting mechanical properties of metal matrix syntactic foams reinforced with ceramic spheres*. Materials Science and Engineering A. 582, 423-432., 2013.
- [6] Ferguson, J. B., Santa Maria, J. A., Schultz, B. F., Gupta, N., Rohatgi, P.K.: *Effect of hollow sphere size and size distribution on the quasi-static and high strain rate compressive properties of Al-A380-Al₂O₃ syntactic foams*. Journal of Materials Science. 49(3), 1267-1278., 2014.
- [7] Weise, J., Lehmhus, D., Baumeister, J., Kun, R., Bayoumi, M., Busse, M.: *Production and Properties of 316L Stainless Steel Cellular Materials and Syntactic Foams*. Steel Research International. 85(3), 486-497., 2013.
- [8] Peroni, L., Scapin, M., Avasse, M., Weise, J., Lehmhus, D., Baumeister, J., Busse M.: *Syntactic iron foams – on deformation mechanisms and strain-rate dependence of compressive properties*. Advanced Engineering Materials. 14, 909-918., 2012.
- [9] Peroni, L., Scapin, M., Avasse, M., Weise, J., Lehmhus, D.: *Dynamic mechanical behavior of syntactic iron foams with glass microspheres*. Materials Science and Engineering A. 552, 364-375., 2012.
- [10] Peroni, L., Scapin, M., Fichera, C., Lehmhus, D., Weise, J., Baumeister, J., Avasse, M.: *Investigation of the mechanical behaviour of AISI 316L stainless steel syntactic foams at different strain-rates*. Composites Part B. 66, 430-442., 2014.
- [11] Taherishargh, M., Belova, I. V., Murch, G. E., Fiedler, T.: *Low-density expanded perlite-aluminium syntactic foam*. Materials Science and Engineering A. 604, 127-134., 2014.
- [12] Taherishargh, M., Belova, I. V., Murch, G. E., Fiedler, T.: *On the mechanical properties of heat-treated expanded perlite-aluminium syntactic foam*. Materials Design. 63, 375-383., 2014.
- [13] Vendra, L., Neville, B., Rabiei, A.: *Fatigue in aluminum-steel and steel-steel composite foams*. Materials Science and Engineering A. 517, 146-153., 2009.
- [14] Hollomet GmbH. www.hollomet.com/home.html, last accessed 5th September 2016.
- [15] ASTM International, ASTM E739-10 (2015) Standard Practice for Statistical Analysis of Linear or Linearized Stress-Life (S-N) and Strain-Life (ε-N) Fatigue Data, ASTM International, West Conshohocken, PA, 2015.
- [16] Envirospheres Pty. Ltd. www.envirospheres.com, last accessed 5th September 2016.